International Journal of Fatigue 32 (2010) 659–669

Contents lists available at ScienceDirect

International Journal of Fatigue

journal homepage: www.elsevier.com/locate/ijfatigue

Influence of the constant life diagram formulation on the fatigue life prediction of composite materials

Anastasios P. Vassilopoulos *, Behzad D. Manshadi, Thomas Keller

Composite Construction Laboratory (CCLab), Ecole Polytechnique Fédérale de Lausanne (EPFL), Station 16, Bâtiment BP, CH-1015 Lausanne, Switzerland

ARTICLE INFO

Article history:
Received 14 May 2009
Received in revised form 3 September 2009
Accepted 4 September 2009
Available online 11 September 2009

Keywords:
Composites
Constant life diagrams
Life prediction
S–N curves
Variable amplitude loading

ABSTRACT

The influence of the constant life diagram (CLD) formulation on the fatigue life prediction of composite materials was examined. Most commonly used and recently proposed CLDs applied on composite materials fatigue data are presented and their applicability on a number of data sets is demonstrated. Composite material fatigue data from a number of well documented databases were used. The influence of the selected CLD formulation on the fatigue life prediction of composite material under spectrum loading is assessed by its ability to accurately predict unknown S–N curves for arbitrary loading. The results revealed that the simple piecewise linear formulation compares favorably to other more sophisticated and complicated schemes. For most of the cases studied, the S–N predictions based on the piecewise linear CLD are the most accurate ones.

1. Introduction

The interpretation of fatigue data constitutes one of the most critical steps in fatigue life prediction methodologies. For those methods that take damage development during fatigue life into account the modeling of a damage metric such as residual strength, residual stiffness, or even actual damage mechanisms like matrix crack density, is essential. For design methodologies that are based on phenomenological modeling and follow theoretical formulations to eventually estimate the fatigue life, the critical points are the S–N type selection, statistical interpretation of fatigue data, selection of the appropriate constant life diagram formulation, fatigue failure criterion, and the damage summation rule [1,2].

Although several effective parameters are introduced in the aforementioned processes, limited efforts have been made to study their effect on fatigue life prediction. For instance, the effectiveness of the Palmgren–Miner rule in comparison with different damage accumulation metrics has been investigated by Bond [1], Philippidis and Vassilopoulos [2] and Hosoi et al. [3]. The role of S–N curve formulation has been studied by Nijssen et al. [4], while the cycle counting effects on the predictions have been considered by Nijssen [5] and Vassilopoulos [6]. Recently, Nijssen [7] has made a broad study of several life prediction parameters on standardized spectra. Likewise, in the most recent investigations, Manshadi et al. [8] developed a software framework for the rapid prototyping of various life prediction schemes in order to validate the influence of different methods for the solution of each step of a classic fatigue life prediction methodology on the resulting lifetime. Cycle counting methods, S–N curve types and different CLD formulations were considered. Passipoularidis and Philippidis [9] have investigated the influence of damage metric selection, constant life diagram (CLD) formulation and cycle counting method on life prediction schemes for composite materials under variable amplitude (VA) loading. This investigation focused on residual strength-based methodologies; different damage functions were implemented and compared with the Palmgren–Miner damage accumulation rule. The predictions were validated by comparison with experimental data from a unidirectional glass/epoxy laminate loaded with three different loading spectra. This investigation also made a limited assessment of the effect of CLD formulation on life prediction.

The classic linear Goodman diagram is the most commonly used CLD, particularly for metals, because of its simplicity. However, it is not suitable for composite materials because of the different tensile and compressive strengths that they exhibit. As a result, a typical CLD for composite materials is shifted to the right hand side and the highest point is located away from the $R = -1, (\sigma_m = 0)$ line. Therefore straight lines connecting the UTS and UCS with points on the $R = -1$ line for different numbers of cycles are not capable to describe the real fatigue behavior of composite materials. Moreover, the damage mechanisms under tension are different to those under compression. In tension, the composite material properties are governed by the fibers, while in compression the properties are mainly determined by the matrix and matrix-fiber interaction.

To cope with these various characteristics of composite materials, several different models have been presented in the literature

* Corresponding author. Tel.: +41 21 6936393; fax: +41 21 6936240.
E-mail address: anastasios.vasilopoulos@epfl.ch (A.P. Vassilopoulos).

0142-1123/$ - see front matter © 2009 Elsevier Ltd. All rights reserved.
doi:10.1016/j.ijfatigue.2009.09.008

[10–22]. Starting from the basic idea of the symmetric and linear Goodman diagram and the non-linear Gerber equation, different modifications were proposed to cover the peculiarities of the behavior of composite materials. Linear interpolation between different S–N curves in a modified Goodman diagram concept was used in several cases [10–12]. Analytical expressions for the theoretical derivation of any desired S–N curve were developed based on this idea [2]. In other proposed models, a minimum of experimental data was used, comparable to the simple Goodman diagram, while simultaneously accommodating the particular characteristics of composites. To this end, a model initially proposed by Dover [13] was introduced by Amijima et al. [14] and Brondsted et al. [15] for composite materials. An alternative semi-empirical formulation was proposed in a series of papers by Harris's group [16–18]. The solution was based on fitting the entire set of experimental data with a non-linear equation to form a continuous bell-shaped line from the ultimate tensile stress to the ultimate compressive stress of the examined material. The drawback of this idea was the need to adjust a number of parameters based on experience and existing fatigue data. Kawai [19–20] proposed the so-called anisomorphic CLD that can be derived by using only one "critical" S–N curve. The critical R-ratio is equal to the ratio of the ultimate compressive over the ultimate tensile stress of the examined material. The obvious drawback of this model is the need for experimental data for this specific S–N curve and therefore, theoretically, it cannot be applied to existing fatigue databases. However, the minimum amount of data required is an asset of the proposed methodology. Based on the Gerber line, another formulation of the CLD has been proposed by Boerstra [21]. This formulation offers a simple method for the lifetime prediction of laminate structures subjected to fatigue load with continuously varying mean stress and dispenses with any classification of fatigue data according to R-values. The disadvantage of this method is the complicated optimization process with five variables that must be followed in order to derive the CLD model. A new model was recently proposed by Kassapoglou [22] is based on the assumption that the probability of failure during any fatigue cycle is constant and equal to the probability of failure under static loading. Based on this assumption, S–N curves under any loading pattern can be derived by using only tensile and compressive static strength data. However, the restricted use of static data ignores the different damage mechanisms that develop during fatigue loading and in many cases leads to erroneous results, e.g., [23]. Novel computational methods were also employed during the last decade for modeling the fatigue behavior of composite materials and the derivation of constant life diagrams based on limited amounts of experimental data, e.g., [24–26]. These methods offer a means of representing the fatigue behavior of the examined composite materials that is not biased by any damage mechanisms and not restricted by any mathematical model description. They are data-driven techniques and their modeling quality depends on the quality of the available experimental data.

This study examines the influence of the constant life diagram formulation on the prediction of the fatigue life of composite materials. The most commonly used and most recent CLD formulations for composite materials are evaluated. The applicability of the models, the need for experimental data and the accuracy of their predictions are considered as critical parameters for the evaluation. The effect of the selection of the CLD formulation on fatigue life prediction is assessed according to its ability to accurately estimate unknown S–N curves. This comparison can also be applied to the life prediction results, but in this case, other parameters that influence the results (S–N curve type, damage summation rule, etc.) may mask the effect of the CLD formulation. Fatigue data from three different glass/polyester material systems are used for the demonstration of the models. Based on the results, recommendations concerning the applicability, advantages and disadvantages of each of the examined CLD formulations are extensively discussed.

2. Theory of CLD models

Constant life diagrams reflect the combined effect of mean stress and material anisotropy on the fatigue life of the examined composite material. Furthermore, they offer a predictive tool for the estimation of the fatigue life of the material under loading patterns for which no experimental data exist. The main parameters that define a CLD are the mean cyclic stress, σ_m, the cyclic stress amplitude, σ_a, and the R-ratio defined as the ratio between the minimum and maximum cyclic stress, $R = \sigma_{min}/\sigma_{max}$. A typical CLD annotation is presented in Fig. 1.

As shown, the positive (σ_m–σ_a)-half-plane is divided into three sectors, the central one comprising combined tensile and compressive loading. The Tension–Tension (T–T) sector is bounded by the radial lines, representing the S–N curves at $R = 1$ and $R = 0$, the former corresponding to static fatigue and the latter to tensile cycling with $\sigma_{min} = 0$. S–N curves belonging to this sector have positive R-values less than unity. Similar comments regarding the other sectors can be derived from the annotations shown in Fig. 1. Every radial line with $0 < R < 1$, i.e., in the T–T sector, has a corresponding symmetric line with respect to the σ_a-axis, which lies in the Compression–Compression (C–C) sector and whose R-value is the inverse of the tensile one, e.g., $R = 0.1$ and $R = 10$.

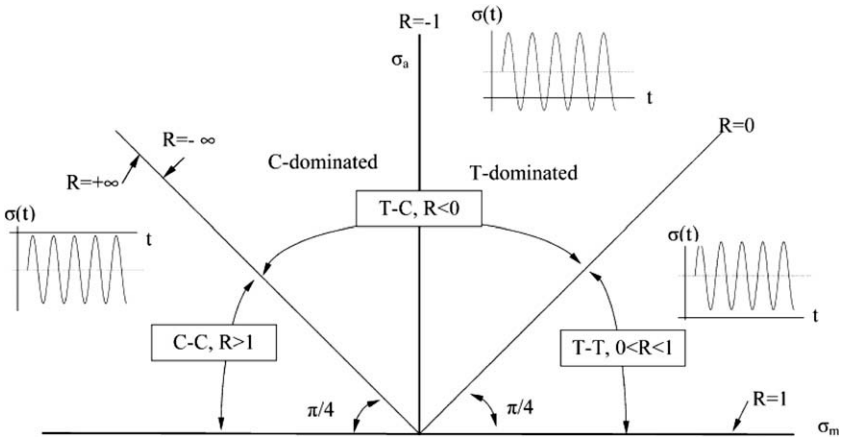

Fig. 1. Annotation for σ_m–σ_a plane [12].

Radial lines emanating from the origin are expressed by:

$$\sigma_a = \left(\frac{1-R}{1+R}\right)\sigma_m \tag{1}$$

and represent a single S–N curve. Points along these lines are points of the S–N curve for that particular stress ratio. Constant life diagrams are formed by joining points of consecutive radial lines, all corresponding to a certain value of cycles.

Although from a theoretical point of view the aforementioned representation of the CLD is rational, it presents a deficiency when seen from the engineering point of view. This deficiency is related to the region close to the horizontal axis, which represents loading under very low stress amplitude and high mean values with a culmination for zero stress amplitude ($R = 1$). The classic CLD formulations require that the constant life lines converge to the ultimate tensile stress (UTS) and the ultimate compressive stress (UCS), regardless of the number of loading cycles. However, this is an arbitrary simplification originating from the lack of information about the fatigue behavior of the material when no amplitude is applied. In fact, this type of loading cannot be considered fatigue loading; but rather creep of the material. (constant static load over a short or long period). Although modifications to account for the time-dependent material strength have been introduced, their integration into CLD formulations requires the adoption of additional assumptions, see e.g., [11,23].

2.1. Linear CLD [13–15]

The linear CLD model is based on a single S–N curve that should be experimentally derived. All other S–N curves can be determined from the given one by simple calculations. This simplified formulation assumes that the failure mechanism is identical in tension and in compression when the load amplitude is the same. In the (σ_m–σ_a)-plane, the above assumption implies that any constant life line forms an isosceles triangle, subtending $\pi/4$ angles with the axes [9]. Any constant life line can be calculated by:

$$\frac{\sigma_a}{\sigma_o} + \frac{\sigma_m}{\sigma_o} = N^{-1/k} \tag{2}$$

where k and σ_o are parameters of the power law equation which describes the S–N curve at the selected R-value.

2.2. Piecewise linear CLD [2]

The piecewise linear CLD is derived by linear interpolation between known values in the (σ_m–σ_a)-plane. This CLD model requires a limited number of experimentally determined S–N curves along with the ultimate tensile and compressive stresses of the materials. S–N curves representing the entire range of possible loading are commonly used for the construction of piecewise linear CLDs, normally at $R = 0.1$ for T–T loading, $R = -1$ for T–C loading and $R = 10$ for C–C loading patterns. Constant life lines connect data points of the same number of cycles on various S–N curves. Unknown S–N curves are calculated by linear interpolation between known values of fatigue and static strength data.

Analytical expressions were developed for the description of each region of the piecewise linear CLD in [2].

1. If R' is in the T–T sector of the CLD, and between $R = 1$ and the first known R-ratio on the (σ_m–σ_a)-plane when moving counterclockwise, R_{1TT}, then

$$\sigma'_a = \frac{\text{UTS}}{\frac{\text{UTS}}{\sigma_{a,1TT}} + r' - r_{1TT}} \tag{3}$$

in which σ'_a and $\sigma_{a,1TT}$ are the stress amplitudes corresponding to R' and R_{1TT}, respectively and $r_i = (1+R_i)/(1-R_i)$, and $r' = (1+R')/(1-R')$.

2. If R' is located between any of two known R-ratios, R_i and R_{i+1},

$$\sigma'_a = \frac{\sigma_{a,i}(r_i - r_{i+1})}{(r_i - r')\frac{\sigma_{a,i}}{\sigma_{a,i+1}} + (r' - r_{i+1})} \tag{4}$$

3. If R' lies in the C–C region of the CLD, and between $R = 1$ and the first known R-ratio in the compression region, R_{1CC},

$$\sigma'_a = \frac{\text{UCS}}{\frac{\text{UCS}}{\sigma_{a,1CC}} - r' + r_{1CC}} \tag{5}$$

where σ'_a and $\sigma_{a,1CC}$ are the stress amplitudes corresponding to R' and R_{1CC}, respectively.

2.3. Harris's CLD [16–18]

Harris and his coworkers developed a semi-empirical equation based on fatigue test data obtained from a range of carbon- and glass-fiber composites [16–18]

$$a = f(1-m)^u(c+m)^v \tag{6}$$

where a is the normalized stress amplitude component, σ_a/UTS, m is the normalized mean stress component, σ_m/UTS, and c is the normalized compression strength, UCS/UTS. In this equation, f, u and v are three adjustable parameters that are functions of fatigue life. Early studies [16–17] showed that parameter f mainly controls the height of the curve, and is a function of the ratio of the compressive to the tensile strength, while the exponents u and v determine the shapes of the two 'wings' of the bell-shaped curve. Initially, the model was established with two simplified forms of Eq. (6) where $u = v = 1$ and $u = v$ for a family of carbon/Kevlar unidirectional hybrid composites [16–17]. However, this model was not accurate for different material systems. Therefore, the general form of Harris's model was implemented in the sequel. In the general form, parameters f, u and v were considered as functions of fatigue life. Depending on the examined material, and the quality of the fatigue data, these parameters were found to depend linearly on the logarithm of fatigue life, log N, for a wide range of FRP materials [18]:

$$\begin{aligned} f &= A_1 \log N + B_1 \\ u &= A_2 \log N + B_2 \\ v &= A_3 \log N + B_3 \end{aligned} \tag{7}$$

in which the parameters A_i and B_i are determined by fitting Eq. (7) to the available experimental data for different loading cycles. Beheshty and Harris [18] showed that the selection of this empirical form for the parameters u and v, can be employed for a wide range of materials, especially CFRP laminates. However, parameter f is extremely sensitive to the examined material and its values vary considerably between GFRP and CFRP laminates. Since, the modeling accuracy of the Harris CLD is significantly dependent on the quality of the fitting of these parameters, Harris and his coworkers established different formulations for the estimation of parameter f based on experimental evidence obtained from a number of different composite material systems. The most recent proposal for the estimation of parameter f is the following equation:

$$f = Ac^{-p} \tag{8}$$

where A and p are functions of log N as well. However, experimental evidence proved that values of $A = 0.71$ and $p = 1.05$ can be used in order to produce acceptable results for a wide range of CFRP and GFRP laminates [16].

2.4. Kawai's CLD [19–20]

Kawai's group developed a formula that describes an asymmetric constant life diagram, designated the anisomorphic constant

fatigue life (CFL) diagram in [19]. The basic characteristic of this formulation is that it can be constructed by using only one experimentally derived S–N, which is called the critical S–N curve. The R-ratio of this S–N curve is defined as the ratio of the ultimate compressive over the ultimate tensile stress of the examined material. The formulation is based on three main assumptions: (i) the stress amplitude, σ_a, for a given constant value of fatigue life N is greatest at the critical stress ratio, (ii) the shape of the CFL curves changes progressively from a straight line to a parabola with increasing fatigue life, and (iii) the diagram is bounded by the static failure envelope, i.e., two straight lines connecting the ultimate tensile and ultimate compressive stresses with the maximum σ_a on the critical S–N curve.

The CFL formulation depends on the position of the mean stress on the (σ_m–σ_a)-plane, whether it is in the tensile or the compressive region. The mathematical formulation reads:

$$\frac{\sigma_a^{\chi}-\sigma_a}{\sigma_a^{\chi}}=\begin{cases}\left(\frac{\sigma_m-\sigma_m^{\chi}}{UTS-\sigma_m^{\chi}}\right)^{(2-\psi_{\chi})}, & UTS \geqslant \sigma_m \geqslant \sigma_m^{\chi}\\ \left(\frac{\sigma_m-\sigma_m^{\chi}}{UCS-\sigma_{m^{\chi}}}\right)^{(2-\psi_{\chi})}, & UCS \leqslant \sigma_m \leqslant \sigma_m^{\chi}\end{cases} \tag{9}$$

where σ_m^{χ} and σ_a^{χ} represent the mean and cyclic stress amplitude for a given constant value of life N under fatigue loading at the critical stress ratio. ψ_{χ} denotes the fatigue strength ratio and is defined as:

$$\psi_{\chi}=\frac{\sigma_{\max}^{\chi}}{\sigma_B} \tag{10}$$

where $\sigma_{\max}^{\chi}$ is the maximum fatigue stress for a given constant value of life N under fatigue loading at the critical stress ratio. σ_B (>0) is the reference strength (the absolute maximum between UTS and UCS) of the material that defines the peak of the static failure envelope. Therefore this normalization guarantees that ψ_{χ} always varies in the range [0, 1] and the exponents $(2-\psi_{\chi})$ in Eq. (9) are always greater than unity. Subsequently, linear $(2-\psi_{\chi}=1)$ or parabolic $(2-\psi_{\chi}>1)$ curves can be obtained from Eq. (9).

The critical fatigue strength ratio represents the normalized cyclic stress, and its relation to the number of loading cycles defines the normalized critical S–N curve:

$$\psi_{\chi}=f^{-1}(2N_f) \tag{11}$$

After determining the critical S–N curve by fitting to the available fatigue data, the CFL diagram can be constructed on the basis of the static strengths, UTS and UCS, and the reference S–N relationship.

Kawai introduced the anisomorphic CFL diagram for the description of the fatigue behavior of CFRP materials.

2.5. Boerstra's CLD [21]

Boerstra [21] proposed an alternative formulation for CLD that can be applied on random fatigue data, which do not necessarily belong to an S–N curve. In this way, the R-ratio is not considered a parameter in the analysis and the model can be applied to describe the behavior of the examined material under loads with continuously changing mean and amplitude values. Boerstra's model constitutes a modification of the Gerber line. The exponent was replaced by a variable also including the difference in tension and compression. The general formulae of the model are:

$$\text{For } \sigma_m>0: \quad \sigma_{ap}=\sigma_{AP}(1-(\sigma_m/\text{UTS})^{\alpha T}) \tag{12}$$

$$\text{For } \sigma_m<0: \quad \sigma_{ap}=\sigma_{AP}(1-(\sigma_m/\text{UCS})^{\alpha C}) \tag{13}$$

where σ_{ap} is the stress amplitude component for a reference number of cycles, N_p, σ_{AP} is an "apex" stress amplitude for N_p and $\sigma_m=0$, and αT and αC are two shape parameters of the CLD curves for the tensile and compressive sides, respectively.

The above equations represent the CLD lines in the (σ_m–σ_a)-plane. According to the author [21], existing fatigue data for different kinds of composite materials show steeper S–N curves under tension and less steep under compression. An exponential relationship with the mean stress can be a good description for the slope $(1/m)$ of S–N lines as follows:

$$m=m_o e^{(-\sigma_m/D)} \tag{14}$$

in which m_o is a measure for the slope of the S–N curve on the log–log scale for $\sigma_m=0$ and D is the skewness parameter for the dependency of m.

Eqs. (12)–(14) suggest that five parameters, m_o, D, N_p, αT, and αC, must be defined in order to construct the CLD model. However, the estimation of the parameters requires a multi-objective optimization process. The aim of this optimization is to estimate the parameters allowing the calculation of the shortest distance between each measuring point and the S–N line for its particular mean stress. The procedure is as follows:

1. The static strengths UTS and UCS are determined and some fatigue test data on coupons with various values of stress amplitude, σ_{α}, and mean stress, σ_m, should also be available.
2. The desired value of N_p is chosen and an initial set of values for parameters m_o, D, N_p, αT, and αC is assumed [21].
3. The slope of the S–N line, m, is calculated for each measured σ_m using Eq. (14).
4. The σ_{α} corresponding to each σ_m is projected to the (σ_m–σ_a)-plane for the selected number of cycles N_p by $\sigma_{ap}=\sigma_a(N/N_p)^{(1/m)}$.
5. σ_{AP}, is calculated for each pair of $\sigma_{\alpha p}$ and σ_m using Eqs. (12) and (13).
6. A modified stress amplitude, $\sigma_{ap,mod}$, is calculated by feeding back the average value of σ_{AP} and the measured mean stress value, σ_m, into Eqs. (12) and (13).
7. The difference between the logarithms of the measured stress amplitude and the modified stress amplitude is then computed as: $\Delta\sigma_{\alpha}=\ln(\sigma_{ap})-\ln(\sigma_{ap,mod})$.
8. The theoretical number of cycles, N_e, corresponding to the $\sigma_{ap,mod}$ stress amplitude and the measured mean stress, σ_m, can be calculated by solving the equation:
$$N_e=N_p\left(\frac{\sigma_{a,mod}}{\sigma_a}\right)^m \tag{15}$$
9. The difference between the measured number of cycles, N, and the theoretical number of cycles, N_e, is defined by $\Delta n=\ln(N)-\ln(N_e)$.
10. The shortest distance between each independent point and the S–N lines in the σ_m–σ_a-N space is expressed by: $\Delta t=sign(\Delta\sigma_a)\sqrt{(1/(1/\Delta\sigma_a^2+1/\Delta n^2))}$. The sum of all Δt's is designated the total standard deviation, SDt. Minimization of the SDt results in the estimation of the optimal m_o, D, N_p, αT, and αC parameters.

2.6. Kassapoglou's CLD [22]

A very simple model was recently proposed by Kassapoglou [22]. Although the model was proposed for the derivation of S–N curves under different R-ratios, it can potentially be used for the construction of piecewise non-linear CLD. The basic assumption of the model is that the probability of failure of the material during a cycle is constant and independent of the current state or number of cycles up to this point. The assumption that the statistical distribution that describes failure under static loading can be used to de-

scribe failure under fatigue loading patterns oversimplifies the reality and masks the effect of the different damage mechanisms that develop under fatigue loading and static loading. However, this model requires no fatigue testing, no empirically determined parameters and no detailed modeling of damage mechanisms.

The model comprises the following equations for calculation of maximum cyclic stress as a function of number of cycles:

$$\sigma_{\max} = \frac{\beta_T}{(N)^{\frac{1}{a_T}}} \quad \text{for } 0 \leqslant R < 1 \tag{16}$$

$$\sigma_{\max} = \frac{\beta_C}{(N)^{\frac{1}{a_C}}} \quad \text{for } R > 1 \tag{17}$$

While for $R < 0$ the following equation should be solved numerically:

$$N = \frac{1}{\left(\frac{\sigma_{\max}}{\beta_T}\right)^{a_T} + \left(\frac{\sigma_{\min}}{\beta_C}\right)^{a_C}} \tag{18}$$

Parameters a_i, β_i, $i = T$, or C denote the scale and shape of a two-parameter Weibull distribution that can describe the static data in tension and compression, respectively.

3. Experimental data

The predicting accuracy of all the examined CLD formulations was assessed on three CA data sets retrieved from three different databases. Fatigue data from tests under tension–tension, tension–compression, and compression–compression loading can be found in these databases. All examined materials are fiberglass-polyester and fiberglass–epoxy laminates, which are typical materials used in the wind turbine rotor blade construction industry.

3.1. Material #1

GFRP multidirectional specimens cut at 45° off-axis from a laminate with the stacking sequence: $[0/(\pm45)_2/0]_T$, [12].

The constant amplitude fatigue of coupons cut at a 45° off-axis angle from a multidirectional laminate with the stacking sequence $[0/(\pm45)_2/0]_T$ was considered as the first example for comparison of the CLD formulations. The material was glass-polyester fabricated using the hand lay-up technique. The selected test set consisted of 57 valid fatigue data points, distributed in four S–N curves (at ratios $R = 0.5$, 0.1, -1 and 10). Tests were conducted at a frequency of 10 Hz. The maximum cyclic stress level ranged between 45 and 130 MPa, and corresponding loading cycles up to failure between 1420 and 3.46 million. Although this data set was relatively limited, it was a typical set of experimental fatigue data for the initial steps of design processes. Details concerning the specified material, preparation and testing procedures can be found in [12]. The UTS for this material was experimentally determined by axial tests as being 139 MPa, while the UCS was estimated as being 106 MPa.

3.2. Material #2

Multidirectional glass-polyester laminate with a stacking sequence that can be encoded as: $[(\pm45)_8/0_7]_S$ [27].

The second material used for the comparisons was a multidirectional glass-polyester laminate consisting of 50% per weight unidirectional and 50 wt% ±45 plies. This configuration can be encoded as $[(\pm45)_8/0_7]_S$. The material data were initially produced for the FACT database and were subsequently included in the OptiDAT database [27]. A total of 101 valid fatigue data points were found for the predetermined material tested under five different constant amplitude conditions: $R = 0.1$, -0.4, -1, 10, -2 and used for comparisons within the framework of this paper. In this data set, the maximum stress level ranged between 65 and 325 MPa and measured lifetime was between 48 for low-cycle fatigue, and 60.3 million cycles for longer lifetimes. A UTS of 370 MPa and a UCS of 286 MPa were reported.

3.3. Material #3

GFRP multidirectional laminate with a stacking sequence of $[90/0/\pm45/0]_S$ [28].

The third example is based on experimental fatigue data retrieved from the DOE/MSU database. The material was a multidirectional laminate consisting of eight layers, six of the stitched unidirectional material D155 and two of the stitched, ±45, DB120. CoRezyn 63-AX-051 polyester was used as the matrix material. In the DOE/MSU database the material has the code name DD16. For constant amplitude fatigue the material was tested under 12 R-ratios for a comprehensive representation of a constant life diagram. Reading counterclockwise on the constant life diagram, the following R-ratios can be identified: 0.9, 0.8, 0.7, 0.5, 0.1, -0.5, -1, -2, 10, 2, 1.43, and 1.1. Here, for comparison of the constant life formulations, experimental data collected under seven R-ratios (0.8, 0.5, 0.1, -0.5, -1, -2, 10) were selected. In total, 360 valid constant amplitude fatigue data points were retrieved from the DOE/MSU database. The absolute maximum stress level during testing was between 85 and 500 MPa and the corresponding recorded cycles up to failure ranged from 37 cycles in the low-cycle fatigue region to 30.4 million in the high cycle fatigue region. More information about this material system and the testing conditions along with more data for further analyses can be found in [28]. The UTS for this material was determined as 632 MPa, while the UCS was 402 MPa.

4. Results and discussion

4.1. Evaluation criteria

The following criteria were considered in order to evaluate the applicability of the examined CLD models and assess their influence on the fatigue life prediction of the examined composite materials:

- Accuracy of predictions: quantified by the accuracy of predicting new S–N curves.
- Need for experimental data: quantified by the number of S–N curves required to form each CLD model.
- Difficulty of application: qualitative criterion.
- Implemented assumptions: qualitative criterion.

All described models were applied on the available fatigue data and the results are presented below. For the application of the linear model, the $R = -1$ curve was used. For the construction of the Kawai CFL, the $R = -1$ curve together with the static strengths were employed. In addition, the $R = -0.5$ curve was used for the modeling of material #3, since for this case the critical R-ratio was -0.63. For the application of the remaining models – piecewise linear, Harris and Boerstra – three to five S–N curves, under $R = 0.1$, $R = -1$, $R = 10$ and additionally $R = 0.5$ and $R = -2$ (for material #3) along with the static strengths were used in order to describe all the regions of the CLD. Kassapoglou's model was applied only for the database of material #3, since it was the only one for which a statistically significant population of static strength data was available.

4.2. Modeling of typical GFRP fatigue data

4.2.1. Material #1

Three of the four existing S–N curves and the static strength values were used as the input data. The S–N curve at $R = -1$ was used for the construction of the linear CLD and the Kawai CFL. The static strength ratio for the examined material according to Kawai is −0.76, but no S–N curve under this R-ratio is available. Power curve fitting was performed on all available experimental fatigue data to determine the S–N curves. These curves were used in all formulations in order to have the same basis for the comparisons. For the model proposed by Boerstra, this is not necessary, as it can be applied even for sparse fatigue data in the $(\sigma_a–\sigma_m–N)$-space. However, the CLD based on the fitted S–N curves was also plotted. Pre-processing of the fatigue data revealed that Eq. (8) is more appropriate for determination of parameter f, as prescribed by the Harris model. Eq. (7) was used for the u and v parameters. The resulting CLD based on the estimation of all parameters using Eq. (7) was also determined for the comparisons.

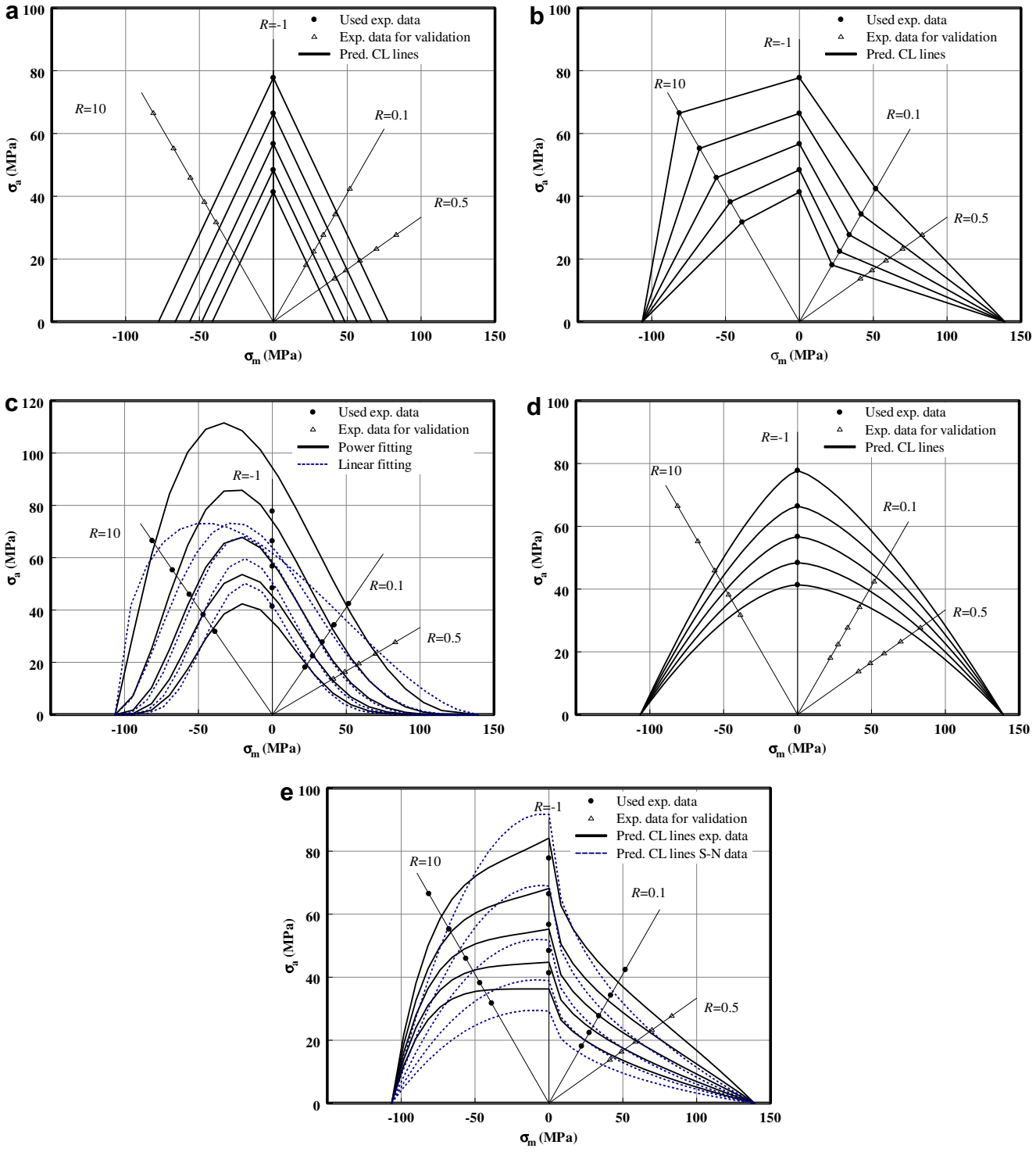

Fig. 2. Constant life diagrams for $N = 10^3 - 10^7$, material #1 (linear-a, piecewise linear-b, Harris-c, Kawai-d, Boerstra-e).

Different CLDs based on the different approaches are presented in Fig. 2. Linear and Kawai CLDs are inaccurate for the examined material, while the prediction of the piecewise linear diagram for the S–N at the stress ratio, $R = 0.5$ is accurate ($R^2 = 0.89$). It has to be mentioned that the S–N curve that has been used as the critical one is different than that recommended by Kawai's model. This difference might be the reason for the inaccurate results. As presented in Fig. 2c, the influence of parameter f on the shape of the predicted CLD based on Harris's model is very important. Insufficient modeling of its relationship to fatigue life can introduce significant errors. However, use of both fitting equations, Eq. (7) or (8), introduced errors, especially close to the low-cycle fatigue region. Application of Boerstra's model based on the experimental results instead of the fitted S–N curves led to a less conservative CLD for the examined material. The accuracy is not significantly affected by this selection however.

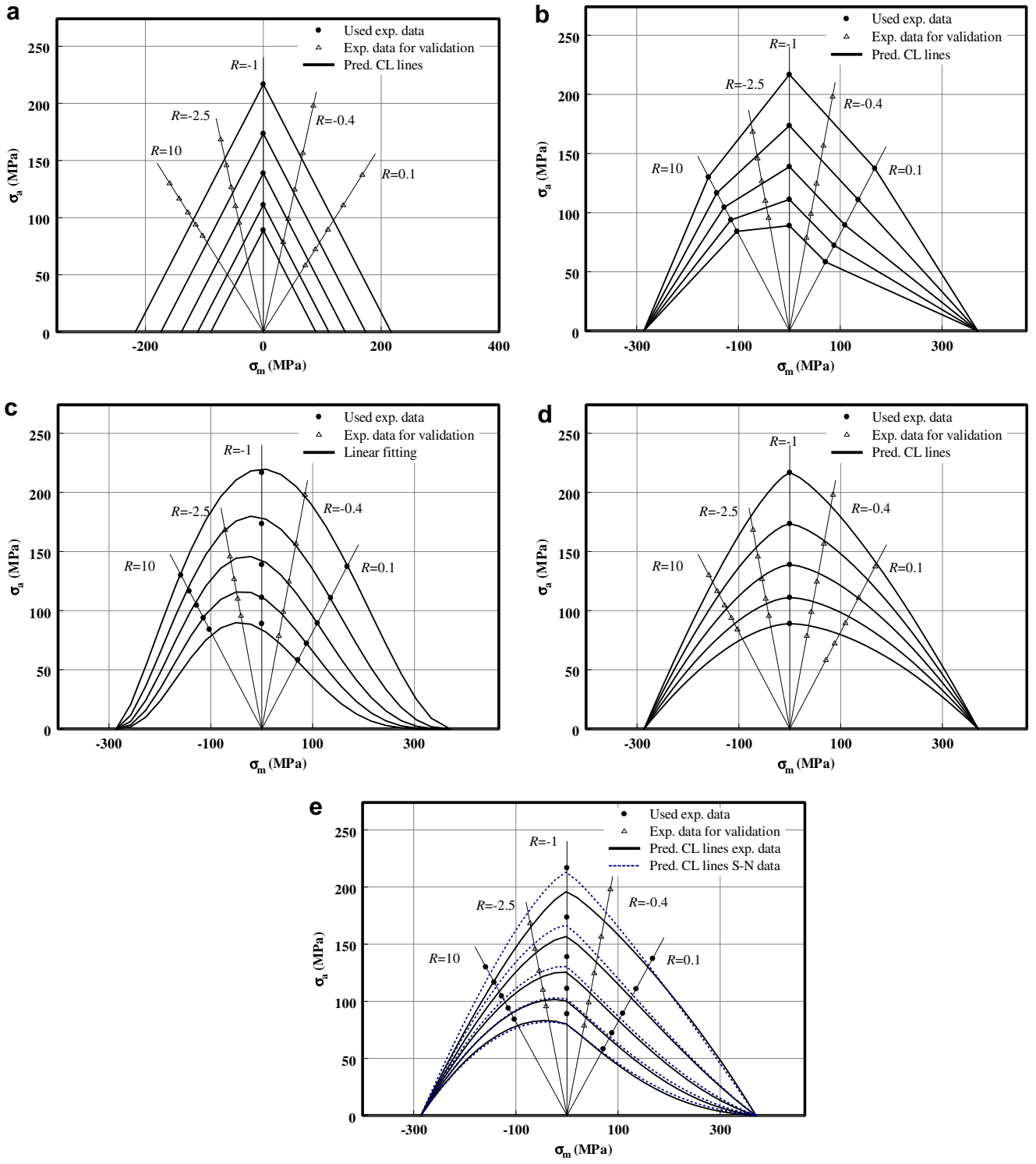

Fig. 3. Constant life diagrams for $N = 10^3 - 10^7$, material #2 (linear-a, piecewise linear-b, Harris-c, Kawai-d, Boerstra-e).

4.2.2. Material #2

Three of the five existing S–N curves plus the static strength values were used as input data. The remaining two were used to evaluate the modeling accuracy of the proposed methods. As for material #1, the $R = -1$ S–N curve was used for the construction of the linear and Kawai models. In the present case, (material #2) the strength ratio equals -0.77. The $R = -1$ curve is the closest one. Based on the pre-processing of the experimental data, all model parameters for Harris were considered as linear functions of the log N and estimated by means of Eq. (7). Log–log S–N curves were derived based on the available data and used as basis for all the mathematical implementations.

Constant life diagrams according to the described models are presented in Fig. 3. All derived CLDs, except that prescribed by the linear model, are accurate for the prediction of the S–N curve at $R = -0.4$ and $R = -2.5$. As can be seen in Fig. 3e, the use of exper-

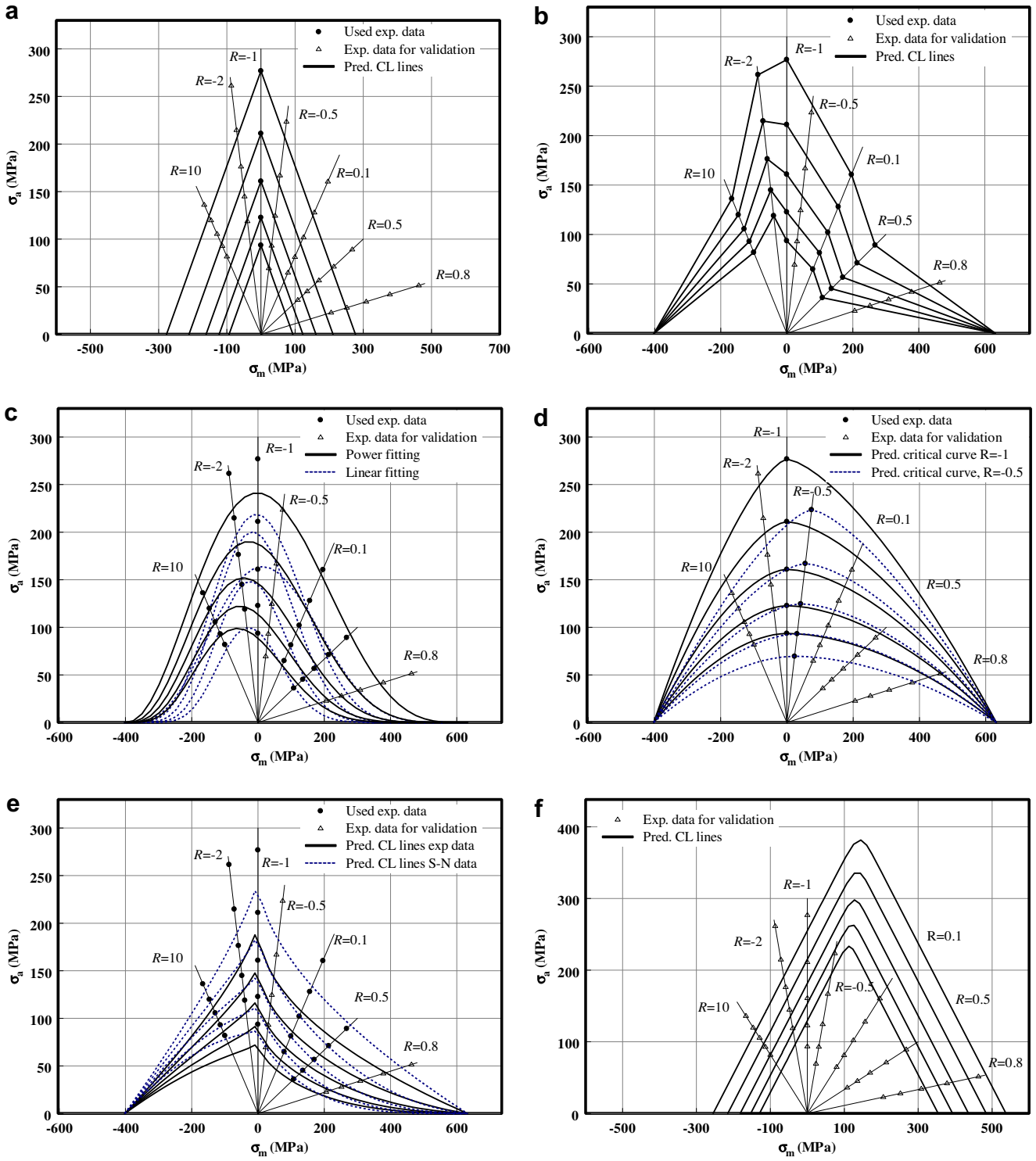

Fig. 4. Constant life diagrams for $N = 10^3 - 10^7$, material #3 (linear-a, piecewise linear-b, Harris-c, Kawai-d, Boerstra-e, Kassapoglou-f).

imental data or fitted S–N data does not significantly affect the predictions based on Boerstra's model. The difference is even less when longer lifetime is evaluated.

4.2.3. Material #3

Five of the seven existing S–N curves plus the static strength values were used as input data for all the CLDs, except for the linear and Kawai models which require only one S–N curve. The remaining two were used to evaluate the modeling accuracy of the proposed methods. For material DD16, the strength ratio according to Kawai is −0.63. Therefore, the S–N curve at $R = -0.5$ was also used for the derivation of the CFL based on Kawai's instructions. Pre-processing of the experimental data showed that the behavior of parameter f in Harris's model can be better fitted by the power law given by Eq. (8). Eq. (7) is used for the other two model parameters. However, application of the model based on the linear fitting of all three parameters was also performed. Power S–N curves were used for the implementation of all models, but again, Boerstra's CLD was constructed using the untreated experimental data as well.

Constant life diagrams according to the described models are presented in Fig. 4. The linear diagram is accurate only for the prediction of the curve at the stress ratio, $R = -0.5$, ($R^2 = 0.93$), but failed to accurately predict the curve at $R = 0.8$. The predictions of the piecewise linear diagram were better in both cases. The influence of the selection of the power or linear fitting for estimation of the parameter f in Harris's model is significant for the examined material, as shown in Fig. 4c. The bad fitting quality of Eq. (7) for the derivation of the relationship between parameter f and number of loading cycles results in the inaccurate CLD that is presented in Fig. 4c. On the other hand, use of the S–N curve at $R = -0.5$, closer to the S–N curve determined as being critical by Kawai, seems to improve the modeling accuracy, although not in a consistent manner. Furthermore, the application of Boerstra's model based on fitted S–N data significantly improved accuracy, especially for the S–N curve at $R = -0.5$. The model proposed by Kassapoglou produced very poor results, although accommodating the very interesting feature of the different static strengths for different loading cycles.

4.3. Evaluation

Comparison of the results shows that the piecewise linear, Harris, Kawai and Boerstra models can be sufficiently accurate under specific conditions. The linear model and the one proposed by Kassapoglou were proved to be inaccurate for the examined material's fatigue data. Comparison of the CLDs from the four eligible models reveals that piecewise linear is more stable that the others since it is not based on any assumption. It is constructed by linear interpolation over the available fatigue data and therefore accurately depicts their behavior. The other three diagrams are very sensitive to the selection of the input data, especially Kawai, and the estimation of the model parameters, e.g., Harris.

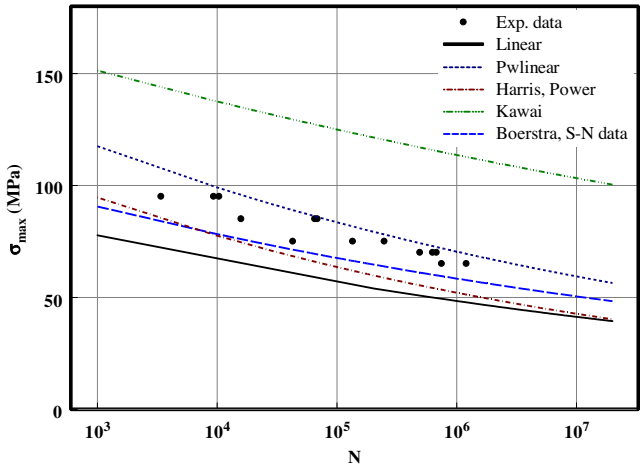

Fig. 6. Predicted S–N curves for $R = 0.5$, material #1.

An attempt for a direct quantitative and qualitative comparison of the constructed CLDs is shown in Fig. 5 for 10^5 cycles and material #3. In this figure, the superiority of the piecewise linear, Harris, and Boerstra models in prediction of the selected points at $R = 0.8$ and $R = -0.5$ against Kawai, linear, and Kassapoglou's models is highlighted. To quantify the result, predicted S–N curves from the different models are presented in Figs. 6–8 and compared to the available experimental data for arbitrarily selected cases. The linear model underestimates the fatigue strength of the examined material in all the examined cases, leading to conservative fatigue life predictions. On the other hand, Kawai's model generally overestimates the behavior, implying an optimistic assessment of fatigue life and thus a non-conservative fatigue design.

A quantification of the predicting ability of each of the applied models was performed. Table 1 shows the R^2 values between the predicted curves and the experimental data for validation. Gener-

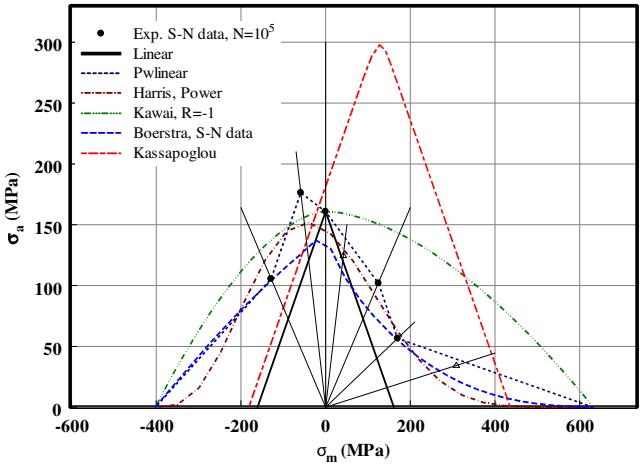

Fig. 5. Comparison of CL lines for 10^5 cycles, material #3.

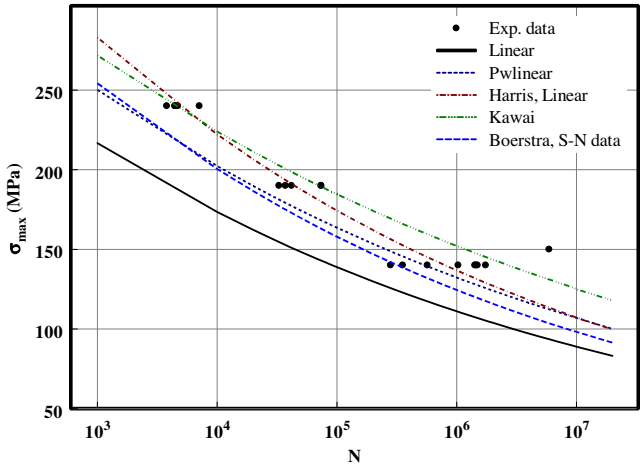

Fig. 7. Predicted S–N curves for $R = -0.4$, material #2.

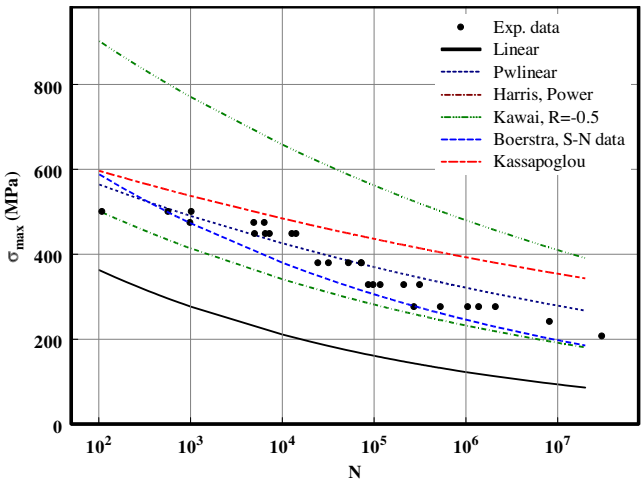

Fig. 8. Predicted S–N curves for $R = 0.8$, material #3.

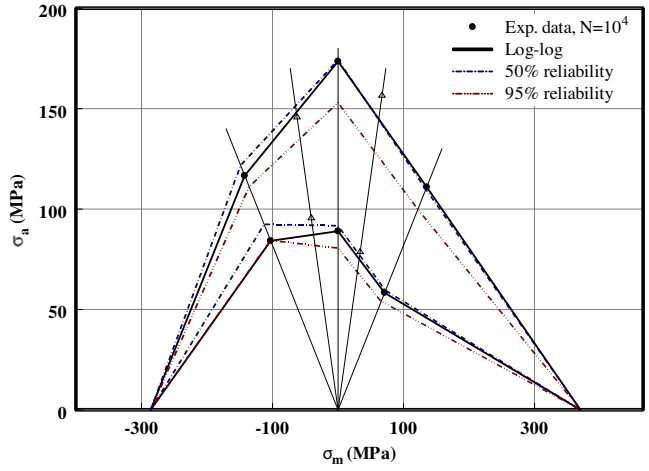

Fig. 9. Comparison of CLDs based on different S–N formulations and different reliability levels, material #2.

Table 1
Comparison of predicting ability of the applied models in terms of the coefficient of multiple determination (R^2).

	Material #1	Material #2		Material #3		
	$R = 0.5$	$R = -0.4$	$R = -2.5$	$R = -1$	$R = -0.5$	$R = 0.8$
Linear	0.37	0.72	0.61	–	0.93	0.35
Piecewise linear	0.89	0.91	0.84	–	0.88	0.93
Harris-f: linear	0.63	0.95	0.71	–	0.77	0.51
Harris-f: power law	0.64	0.94	0.64	–	0.94	0.80
Kawai ($R = -1$)	0.15	0.94	0.83	–	0.87	0.31
Kawai ($R = -0.5$)	–	–	–	0.76	–	0.43
Boerstra-experimental data	0.65	0.86	0.83	–	0.60	0.85
Boerstra-S–N data	0.69	0.89	0.84	–	0.84	0.91
Kassapoglou	–	–	–	0.93	0.41	0.48

ally higher values were exhibited by the piecewise linear. This model seems to be the most reliable for the entire set of data examined in the present paper. Other CLD formulations can also be accurate however, although not consistently so. Their accuracy depends on the quality of the examined fatigue data, the selected input data (e.g., linear, Kawai) and the quality of the fitting and/or optimization for estimation of the parameters (Harris and Boerstra).

In terms of need for experimental data, it is obvious that the model proposed by Kassapoglou is the least demanding, followed by the linear and Kawai models. However, as already discussed, this compromise hinders the accuracy of the predictions. Piecewise linear can also be implemented by using a single S–N curve, thus representing the Goodman diagram, but, as mentioned above, in this case its predictive ability is also reduced.

As far as ease of application is concerned, the only difficulty occurs in the Harris and Boerstra models. According to the former, a non-linear regression should be performed for the derivation of the three model parameters, while for the latter, a five-parameter optimization problem must be solved to estimate desired constant life lines.

Apart from the piecewise linear, all other models depend on a number of assumptions. These assumptions originate either from experience and experimental evidence, e.g., in the linear, Harris, Kawai, and Boerstra models, or are clearly theoretical assumptions like the one introduced by Kassapoglou. As previously shown, the adoption of any assumption can give simplicity to the models, which, under certain conditions, can produce quite accurate results. However, there is no guarantee that these models can be used for different materials or even different loading patterns.

All derived CLDs are based on the assumption that a power curve (log–log S–N) is appropriate for the fitting of the fatigue data. If a different formulation is used for interpretation of the fatigue data, the results will be different. Furthermore, mean values of fatigue data were used, i.e., the "mean" S–N curves were employed for the construction of the CLDs. Any other formulation can obviously be employed for interpretation of the fatigue data, e.g., a mathematical expression that provides statistically based S–N curves [29] or even S–N curves estimated by using computational tools such as genetic programming [25] or neural networks [24]. The piecewise linear CLD for material #2 would look like that shown in Fig. 9, if S–N curves for 50% and 95% reliability levels as derived based on the method described in [29] are used for interpretation of the fatigue data.

As can be seen, use of a different S–N formulation has a limited effect on the CLD shape, especially for numbers of cycles between 10^3 and 10^7. As was shown in [25], in this region most S–N formulations provide similar fatigue models. Higher reliability imposes more conservative diagrams however.

5. Conclusions

A comparison of the commonly used and recently developed models for derivation of constant life diagrams for composite materials was carried out in this paper. Six methods were described, and their prediction accuracy was evaluated over a wide range of constant amplitude fatigue data from GFRP materials. The influence of the selection of the CLD method on the fatigue life prediction of composite materials was quantified. The following conclusions were drawn:

- The selection of an accurate CLD formulation is essential for the overall accuracy of a fatigue life prediction methodology. As shown, the "wrong" choice can produce very conservative or very optimistic S–N curves, which is directly reflected in the corresponding life assessment.
- All methods entail the problem of mixing static and fatigue data. Their accuracy is reduced when curves close to $R = 1$ (in tension or compression) have to be predicted. Moreover, the same applies for the derivation of accurate S–N curves to describe the very low-cycle fatigue regime, i.e., $N < 100$. The unified equa-

tion that is used in Harris's model to describe the fatigue behavior for both tension and compression loading combines also the influence of the damage mechanisms that developed under different loading patterns. All other models work separately for tension and compression loading; they are based on different equations for the description of different parts of the constant life diagram.

- The simplicity offered by some of the models, e.g., linear, Kassapoglou, Kawai, in most cases compromises accuracy. In addition, although these models were developed with the aim of minimizing the amount of experimental data required, they do not offer the possibility of using more data when an extensive database is available, e.g., linear and Kawai are based on the critical S–N curve and cannot accommodate any other S–N curve in order to improve the accuracy of the predictions. Another deficiency of models like these two is that they cannot be used to analyze random variable amplitude fatigue loading with continuously changing mean and amplitude, since they are accurate only for S–N curves close to the critical one (for the linear) and only if the critical one (according to the material) can be experimentally derived (Kawai). It should be mentioned however, that Kawai introduced his model for the description of CFRP material behavior different to that of the GFRP materials examined in this study.
- The accuracy of Harris's model is acceptable only when the behavior of the model parameters can be effectively fitted versus the fatigue life. However, the fitting methods proposed by Harris do not always lead to accurate results.
- Boerstra's model can be used without the need to fit the available experimental data with an S–N curve. This is an asset since it can therefore be used to model variable amplitude data with continuously varying mean and amplitude values. However, it was proved that use of the fitted S–N data instead improves the modeling accuracy of the Boerstra model.
- The relatively simple piecewise linear was proved the most accurate of the compared formulations when a reasonable number of S–N curves (>3) is available. A more sophisticated, nonlinear interpolation between the known S–N values and a more realistic description of the behavior close to $R = 1$ would improve the results of this model.

References

[1] Bond IP. Fatigue life prediction for GRP subjected to variable amplitude fatigue. Compos: Part A 1999;30(8):961–70.
[2] Philippidis TP, Vassilopoulos AP. Life prediction methodology for GFRP laminates under spectrum loading. Compos: Part A 2004;35(6):657–66.
[3] Hosoi A, Kawada H, Yoshino H. Fatigue characteristics of quasi-isotropic CFRP laminates subjected to variable amplitude cyclic two stage loading. Int J Fatigue 2006;28(10):1284–9.
[4] Nijssen RPL, van Delft DRV, van Wingerde AM. Alternative fatigue lifetime prediction formulations for variable amplitude loading. J Sol Energy, Trans ASME 2002;124(4):396–403.
[5] Nijssen RPL. (NEW) WISPER(X) load spectra. Test results and analysis. OB_TG1_R024; 2005. 10p. <http://www.kc-wmc.nl/optimatblades/Publications>.
[6] Vassilopoulos AP. A new software framework for fatigue life prediction of composite materials under irregular loading. Adv Compos Lett 2006;15(1):23–9.
[7] Nijssen RPL. Fatigue life prediction and strength degradation of wind turbine rotor blade composites. PhD thesis, TU Delft; 2006.
[8] Manshadi BD, Vassilopoulos AP, Keller T. A computational tool for the fatigue life prediction of composite materials, In: Proceedings of the 2nd international conference on material and component performance under variable amplitude loading, Darmstadt, Germany, 23–26 March; 2009. p. 585–94.
[9] Passipoularidis VA, Philippidis TP. A study of factors affecting life prediction of composites under spectrum loading. Int J Fatigue 2009;31(3):408–17.
[10] Mandell JF, Samborsky DD, Wang L, Wahl NK. New fatigue data for wind turbine blade materials. J Sol Energy Eng, Trans ASME 2003;125(4):506–14.
[11] Sutherland HJ, Mandell JF. Optimized constant life diagram for the analysis of fiberglass composites used in wind turbine blades. J Sol Energy Eng, Trans ASME 2005;127(4):563–9.
[12] Philippidis TP, Vassilopoulos AP. Complex stress state effect on fatigue life of GFRP laminates. Part I, experimental. Int J Fatigue 2002;24(8):813–23.
[13] Dover WD. Variable amplitude fatigue of welded structures. In: Smith RA, editor. Fracture mechanics: current status future prospects. Cambridge: Pergamon Press; 1979. p. 125–47.
[14] Amijima S, Tanimoto T, Matsuoka T. A study on the fatigue life estimation of FRP under random loading. In: Hayashi T, Kawata K, Umekawa S, editors. Progress in science and engineering of composites. Berlin; 1982. p. 701–8.
[15] Brondsted P, Andersen SI, Lilholt H. Fatigue damage accumulation and lifetime prediction of GFRP materials under block loading and stochastic loading. In: Andersen SI, Brondsted P, et al., editors. Proceedings of the 18th risoe international symposium on material science; 1997. p. 269–78.
[16] Harris B. A parametric constant-life model for prediction of the fatigue lives of fibre-reinforced plastics. In: Harris B, editor. Fatigue in composites. Woodhead Publishing Limited; 2003. p. 546–68.
[17] Gathercole N, Reiter H, Adam T, Harris B. Life prediction for fatigue of T800/5245 carbon fiber composites: I. Constant amplitude loading. Int J Fatigue 1994;16(8):523–32.
[18] Beheshty MH, Harris B. A constant life model of fatigue behavior for carbon fiber composites: the effect of impact damage. Compos Sci Technol 1998;58(1):9–18.
[19] Kawai M, Koizumi M. Nonlinear constant fatigue life diagrams for carbon/epoxy laminates at room temperature. Compos: Part A 2007;38(11):2342–53.
[20] Kawai M. A method for identifying asymmetric dissimilar constant fatigue life diagrams for CFRP laminates. Key Eng Mater 2007;334–335:61–4.
[21] Boerstra GK. The multislope model: a new description for the fatigue strength of glass reinforced plastic. Int J Fatigue 2007;29(8):1571–6.
[22] Kassapoglou C. Fatigue life prediction of composite structures under constant amplitude loading. J Compos Mater 2007;41(22):2737–54.
[23] Awerbuch J, Hahn HT. Off-axis fatigue of graphite/epoxy composite. Fatigue of fibrous composite materials, ASTM STP 723. American Society for Testing and Materials; 1981. p. 243–73.
[24] Vassilopoulos AP, Georgopoulos GF, Dionyssopoulos V. Artificial neural networks in spectrum fatigue life prediction of composite materials. Int J Fatigue 2007;29(1):20–9.
[25] Vassilopoulos AP, Georgopoulos EF, Keller T. Comparison of genetic programming with conventional methods for fatigue life modeling of FRP composite materials. Int J Fatigue 2008;30(9):1634–45.
[26] Silverio Freire RC, Dória Neto AD, De Aquino EMF. Comparative study between ANN models and conventional equation in the analysis of fatigue failure of GFRP. Int J Fatigue 2009;31(5):831–9.
[27] Nijssen RPL. OptiDAT – fatigue of wind turbine materials database; 2006. <http://www.kc-wmc.nl/optimat_blades/index.htm>.
[28] Mandell JF, Samborsky DD. DOE/MSU composite material fatigue database. Sandia National Laboratories, SAND97-3002. <http://www.sandia.gov/wind> [v. 18, updated 21:03:08].
[29] Sendeckyj GP. Fitting models to composite materials fatigue data. In: CC CHAMIS, editor. Test methods and design allowables for fibrous composites, ASTM STP 734. American Society for Testing and Materials; 1981. p. 245–60.